

# Communications Research Centre

COMMUNICATIONS CANADA  
MAR 11 1982  
LIBRARY - BIBLIOTHÈQUE

## ADAPTIVE JAMMER SUPPRESSION BY ORTHONORMALIZATION

by

E.K.L. Hung and R.M. Turner

IC

This work was sponsored by the Department of National Defence, Research and Development Branch under Project No. 33C69.

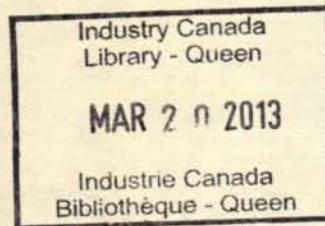
LKC  
TK  
5102.5  
.R48e  
#706  
c.2

DEPARTMENT OF COMMUNICATIONS  
MINISTÈRE DES COMMUNICATIONS

CRC TECHNICAL NOTE NO. 706

COMMUNICATIONS RESEARCH CENTRE

DEPARTMENT OF COMMUNICATIONS  
CANADA



ADAPTIVE JAMMER SUPPRESSION BY ORTHONORMALIZATION

by

E.K.L. Hung and R.M. Turner

*(Radar and Communications Technology Branch)*



CRC TECHNICAL NOTE NO. 706

May 1981  
OTTAWA

This work was sponsored by the Department of National Defence, Research and Development Branch under Project No. 33C69.

CAUTION

The use of this information is permitted subject to recognition of  
proprietary and patent rights.

1950  
MAY 10 1950  
U.S. AIR FORCE  
COMMUNICATIONS CENTER  
WASH. D.C.

RECEIVED  
MAY 10 1950  
COMMUNICATIONS CENTER  
U.S. AIR FORCE  
WASH. D.C.

TK  
5102.5  
R48e  
#706  
C.10

TABLE OF CONTENTS

ABSTRACT . . . . . 1

1. INTRODUCTION . . . . . 1

2. ALGORITHM . . . . . 2

    2.1 Assumptions . . . . . 2

    2.2 Theory . . . . . 2

    2.3 Procedure . . . . . 4

    2.4 Computation Count . . . . . 5

3. COMPUTER SIMULATIONS . . . . . 6

    3.1 Equations . . . . . 6

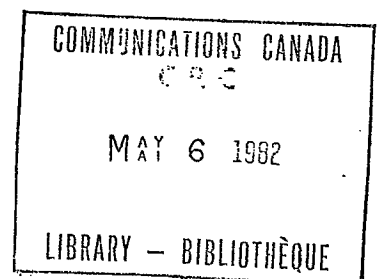
    3.2 Simulation 1 . . . . . 7

    3.3 Simulation 2 . . . . . 11

    3.4 Simulation 3 . . . . . 12

4. CONCLUSIONS . . . . . 12

5. ACKNOWLEDGEMENT . . . . . 14



# ADAPTIVE JAMMER SUPPRESSION BY ORTHONORMALIZATION

by

E.K.L. Hung and R.M. Turner

## ABSTRACT

*This jammer suppression algorithm is written specifically for array radars in which the number of array elements  $K$  is very large compared with the number of jammers  $L$  the radar is designed to suppress. It separates the quiescent weight vector into two components. The component orthogonal to a set of  $M$  noise sample vectors is renormalized to unit length and identified as the adapted weight vector.*

*This algorithm is effective in the suppression of many types of jammers, including repeater and blinker jammers. The number of noise samples required in the construction of the adapted weight vector is usually very small. In the special case of  $L$  monotone jammers, for example, a choice  $M=L$  usually reduces output jammer power to a few dB above the white noise background. It is permissible to set  $M < L$ . In this case, the first  $M$  strongest jammers are given the most suppression.*

*This algorithm requires  $(4M^2+6M+2)K$  real add,  $(4M^2+8M+4)K$  real multiply,  $(M+1)$  real square root, and  $(M+1)$  real divide operations. Almost all of these computer operations are in the form of vector operations.*

## 1. INTRODUCTION

An adaptive jammer suppression algorithm based on the Gram-Schmidt orthonormalization method is described in this Technical Note. The derivation of this technique is given in Section 2. Computer simulations to study the properties of this algorithm can be found in Section 3.

## 2. ALGORITHM

The assumptions in the derivation of the adaptive jammer suppression algorithm are written down. Vectors representing antenna output, noise jammers, and noise samples are introduced. From the relations among these vectors, a technique to construct an adaptive weight vector for the array elements is derived. The procedure for the computation of this weight vector is then presented. Finally, an estimation on the computation requirements of this algorithm is made.

### 2.1 ASSUMPTIONS

The assumptions are as follows:

1. Noise jammers are mutually uncorrelated.
2. The changes in jammer directions are negligible during adaptation and radar amplitude measurement.

### 2.2 THEORY

Let  $K$  denote the number of elements in the radar antenna. Each sampling of the environment by this radar produces a sampling vector  $\underline{r} = (r_1, r_2, \dots, r_K)$ , where  $r_k$  is the quadrature sampled output of the  $k^{\text{th}}$  array element. Radar output power is constructed as

$$P = |(\underline{w}, \underline{r})|^2, \quad (1)$$

where  $\underline{w} = (w_1, w_2, \dots, w_K)$  is a vector of weighting coefficients for the array element outputs, and

$$(\underline{w}, \underline{r}) = \sum_{k=1}^K w_k^* r_k \quad (2)$$

is the scalar product of  $\underline{w}$  and  $\underline{r}$ .

The value of  $P$  given by eqn. (1) is proportional to  $|\underline{w}|^2$ . For the sake of convenience in the comparison of radar output power constructed with different weight vectors, it is useful to impose the condition

$$\begin{aligned} |\underline{w}|^2 &= (\underline{w}, \underline{w}) \\ &= 1. \end{aligned} \quad (3)$$

This normalization of  $\underline{w}$  to unit length has a very useful property. In the presence of white noise only, the sampling vector is given by  $\underline{r} = \underline{\eta} = (\eta_1, \eta_2, \dots, \eta_K)$ , where the  $\eta_k$ 's are mutually uncorrelated array element output amplitudes with zero mean and variance  $\sigma_\eta^2$ . The expected value of  $P$  with white noise input is



$$E\{P\} = E \left\{ \sum_{k=1}^K w_k^* \eta_k \sum_{k'=1}^K w_{k'} \eta_{k'}^* \right\}$$

$$= \sigma_\eta^2 . \quad (4)$$

This expected value is the expected value of white noise power at the array elements.

In general, sampling vector  $\underline{r}$  is a sum of three components,

$$\underline{r} = \underline{s} + \underline{g} + \underline{\eta} \quad (5)$$

where  $\underline{s}$  is the signal component,  $\underline{g}$  is the jammer component, and  $\underline{\eta}$  is the white noise component. The quiescent weight vector is defined as

$$\underline{w}_q = \frac{\underline{s}}{|\underline{s}|} . \quad (6)$$

This vector maximizes the output signal power in  $P_q = |(\underline{w}_q, \underline{r})|^2$  by match filtering and is the optimal weight vector in the absence of jammers (i.e.,  $\underline{g}=0$ ). With jammers present,  $\underline{w}_q$  is not the optimal weight vector. It is possible to construct a weight vector, denoted by  $\underline{w}_a$ , such that  $P_a = |(\underline{w}_a, \underline{r})|^2$  has better signal detection properties than  $P_q$ .

The objective of the jammer suppression algorithm here is to construct a weight vector  $\underline{w}_a$  by adaptation such that

$$\underline{w}_a = \frac{\underline{w}_q^\circ}{|\underline{w}_q^\circ|} , \quad (7)$$

where  $\underline{w}_q^\circ$  is the component of  $\underline{w}_q$  orthogonal to a subspace spanned by the jammer vectors. It can easily be verified that

$$(\underline{w}_q^\circ, \underline{r}) = (\underline{w}_q, \underline{r}^\circ) \quad (8)$$

where  $\underline{r}^\circ$  is the component of  $\underline{r}$  orthogonal to the same subspace spanned by the jammer vectors.

Let  $\{\underline{u}_1, \underline{u}_2, \dots, \underline{u}_M\}$  be a set of  $M$  sampling vectors measured with the signal absent (i.e.,  $\underline{s}=0$ ). In Section 2.3, it is shown that these vectors can be used to construct a set of mutually orthogonal vectors  $\{\underline{v}_1, \underline{v}_2, \dots, \underline{v}_M\}$ , where each vector in this set is either a unit vector or a null vector  $\underline{0} = (0, 0, \dots, 0)$ . The non-zero vectors in this set are now treated as basis vectors in a subspace spanned by the jammer vectors. Vector  $\underline{w}_q^\circ$  can be constructed by removing the component of  $\underline{w}_q$  in this subspace. Vector  $\underline{w}_a$  can be calculated with  $\underline{w}_q^\circ$  and eqn. (7).

## 2.3 PROCEDURE

The computation of adapted weight vector  $\underline{w}_a$  is divided into eleven steps. The technique used to calculate  $\{\underline{v}_1, \underline{v}_2, \dots, \underline{v}_M\}$  is modified from the Gram-Schmidt orthonormalization method. Here, a threshold  $\Delta$  is introduced to decide whether a vector should be treated as a jammer vector or as a sum of a white noise vector plus errors introduced by quantization, finite word length of computer storages, etc.. The details in the calculation of  $\underline{w}_a$  are given below:

Step 1 Calculate  $|\underline{u}_1|^2$

Step 2 Calculate  $\underline{v}_1$  as

$$\underline{v}_1 = \begin{cases} \underline{u}_1 / |\underline{u}_1|, & |\underline{u}_1|^2 \geq \Delta, \\ 0, & |\underline{u}_1|^2 < \Delta. \end{cases} \quad (9)$$

Step 3 Set  $m=2$ .

Step 4 Calculate  $\underline{u}'_m$  as

$$\underline{u}'_m = \underline{u}_m - \sum_{m'=1}^{m-1} (\underline{u}_m, \underline{v}_{m'}) \underline{v}_{m'} \quad (10)$$

Step 5 Calculate  $|\underline{u}'_m|^2$

Step 6 Calculate  $\underline{v}_m$  as

$$\underline{v}_m = \begin{cases} \underline{u}'_m / |\underline{u}'_m|, & |\underline{u}'_m|^2 \geq \Delta, \\ 0, & |\underline{u}'_m|^2 < \Delta. \end{cases} \quad (11)$$

Step 7 If  $m=M$ , proceed directly to Step 10.

Step 8 Replace  $m$  by  $m+1$ .

Step 9 Return to Step 4.

Step 10 Calculate  $\underline{w}_q^0$  as

$$\underline{w}_q^0 = \underline{w}_q - \sum_{m=1}^M (\underline{w}_q, \underline{v}_m) \underline{v}_m \quad (12)$$

Step 11 Calculate  $\underline{w}_a$  as

$$\underline{w}_a = \frac{\underline{w}_q^0}{|\underline{w}_q^0|} \quad (7')$$



## 2.4 COMPUTATION COUNT

A rough estimate on the number of computer operations in each step of the algorithm procedure is given below

- Step 1     $2K$  add +  $2K$  multiply to calculate  $|\underline{u}_1|^2$ .
- Step 2    One  $\sqrt{\quad}$  to calculate  $|\underline{u}_1|$ .  
           One divide to calculate  $1/|\underline{u}_1|$ .  
            $2K$  multiply to calculate  $\underline{u}_1/|\underline{u}_1|$ .
- Step 3    Essentially zero
- Step 4     $4(M-1)MK$  add +  $4(M-1)MK$  multiply.  
           Each  $(\underline{u}_m, \underline{v}_m)$  requires  $4K$  add +  $4K$  multiply.  
           Subtraction of  $(\underline{u}_m, \underline{v}_m) \underline{v}_m$  from  $\underline{u}_m$  requires  $4K$  add  
           +  $4K$  multiply also. The ranges for  $m$  and  $m'$  are  
            $2 \leq m \leq M$  and  $1 \leq m' \leq m-1$ .
- Step 5     $2(M-1)K$  add +  $2(M-1)K$  multiply.  
           Each  $|\underline{u}'_m|^2$  requires  $2K$  add +  $2K$  multiply.
- Step 6     $(M-1) \sqrt{\quad}$  +  $(M-1)$  divide +  $2(M-1)K$  multiply.
- Step 7    Essentially zero.
- Step 8    Essentially zero.
- Step 9    Zero
- Step 10    $8MK$  add +  $8MK$  multiply
- Step 11    $2K$  add +  $2K$  multiply + one  $\sqrt{\quad}$  + one divide to calculate  
            $1/|\underline{w}_q^\circ|$ .  
            $2K$  multiply to calculate  $\underline{w}_q^\circ/|\underline{w}_q^\circ|$ .

The sum total is  $(4M^2+6M+2)K$  add +  $(4M^2+8M+4)K$  multiply +  $(M+1)$  square root +  $(M+1)$  divide operations. Given  $M$ , the number of add and multiply operations are proportional to  $K$  only.

### 3. COMPUTER SIMULATIONS

Three simulations were carried out to study the manner in which jammers were suppressed, the performance of the algorithm in the presence of a band jammer, and the performance in the presence of a cluster of jammers.

#### 3.1 EQUATIONS

The array chosen for study was a linear array as shown in Figure 1. There were ten isotropic elements (i.e.,  $K=10$ ) spaced at a distance of half a wavelength. The quiescent beam pointing direction  $\theta_q$  was arbitrarily chosen to be the broadside direction (i.e.,  $\theta_q=0$ ). The quiescent weight vector  $\underline{w}_q = (w_{q1}, w_{q2}, \dots, w_{qK})$  was calculated as

$$\begin{aligned} w_{qk} &= \frac{1}{\sqrt{K}} e^{j\pi k \sin\theta_q} \\ &= \frac{1}{\sqrt{K}}, \quad k = 1, 2, \dots, K. \end{aligned} \quad (13)$$

Each vector in  $\{\underline{u}_1, \underline{u}_2, \dots, \underline{u}_M\}$  was calculated as a sum of a jammer vector and a white noise vector:

$$\underline{u}_m = \underline{g}_m + \underline{n}_m, \quad m = 1, 2, \dots, M. \quad (14)$$

The components of  $\underline{g}_m = (g_{m1}, g_{m2}, \dots, g_{mK})$  were calculated as

$$\begin{aligned} g_{mk} &= \sum_{\ell=1}^L \sqrt{P_\ell} e^{j\phi_{\ell m}} e^{j\pi k f_\ell \sin\theta_\ell}, \\ &k = 1, 2, \dots, K. \end{aligned} \quad (15)$$

Here,  $L$  was the number of jammers,  $P_\ell$  was the power of the  $\ell^{\text{th}}$  jammer at the array elements,  $\phi_{\ell m}$  was a phase constant extracted from a population uniformly distributed in the range  $(-\pi, \pi]$ ,  $f_\ell$  was the jammer frequency relative to the radar design frequency, and  $\theta_\ell$  was the jammer direction. The components of white noise vector  $\underline{n}_m = (n_{m1}, n_{m2}, \dots, n_{mK})$  were generated with the following properties:

$$E\{\text{Re}(n_{mk})\} = E\{\text{Im}(n_{mk})\} = 0 \quad (16)$$

$$\text{var}\{\text{Re}(n_{mk})\} = \text{var}\{\text{Im}(n_{mk})\} = 0.5 \sigma_\eta^2. \quad (17)$$

Here,  $\text{Re}\{n_{mk}\}$  and  $\text{Im}\{n_{mk}\}$  were the real and imaginary components of  $n_{mk}$  respectively, and  $\sigma_\eta^2$  was the white noise power at the array elements.

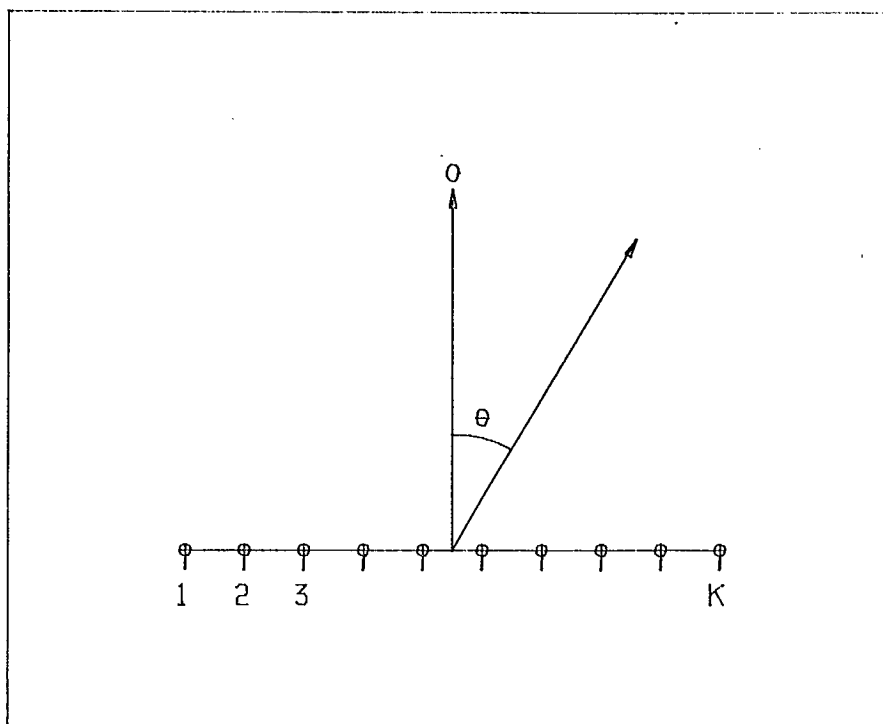


Figure 1. Array configuration in computer simulations. The broadside direction is the zero degree direction. Angle  $\theta$  is measured clockwise from the broadside direction.

Array gain  $G(\theta)$  was defined as

$$G(\theta) = |(\underline{w}, \underline{s})|^2, \quad (18)$$

where the components of  $\underline{s} = (s_1, s_2, \dots, s_K)$  were

$$s_k = e^{j\pi k f \sin \theta}, \quad k = 1, 2, \dots, K \quad (19)$$

and  $f$  was the relative frequency at which the gain was calculated.

### 3.2 SIMULATION 1

This simulation studied the manner in which the jammers were suppressed as the number of noise samples was increased. The parameters for the number of array elements, quiescent beam pointing direction, and frequency for the calculation of array gain were  $K=10$ ,  $\theta_d=0^\circ$ , and  $f=1.0$ . White noise power was arbitrarily chosen as  $\sigma_n^2 = 10^{-4}$ . Its actual value was of no importance here, because it was only used as a reference for power ratios. The jammer parameters were  $L=3$ ,  $(P_1, P_2, P_3) = (1, 0.1, 0.01)$ ,  $(f_1, f_2, f_3) = (1, 1, 1)$ , and  $(\theta_1, \theta_2, \theta_3) = (-17, 30, 65)$  degrees. These parameters corresponded to the presence of three jammers at the radar frequency. The jammer powers were 40, 30, and 20 dB above  $\sigma_n^2$ . Their directions were quite close to three of the sidelobe peaks of the quiescent beam pattern. Threshold in eqn. (9) was calculated as

$$\Delta = 4K\sigma_{\eta}^2 \quad (20)$$

Computer simulations were carried out with  $M=0,1,2$ , and 3 for the number of noise vectors. With these values of  $M$ , the dependence of array gain and jammer suppression on the number of noise vectors was studied.

Presented in Figure 2 is the quiescent gain pattern  $G(\theta)$  calculated at  $0.5^\circ$  intervals with  $M=0$ . Here, the beam pointing direction,  $\theta_q$  is marked with an arrow just above  $G(\theta_q)$ , and  $G(\theta_q)$  was 10.00 dB. The jammer positions are marked with arrows below the X-axis. In Table 1, the gains in the directions of the jammers were  $G(\theta_1) = -3.00$  dB,  $G(\theta_2) = -6.99$  dB and  $G(\theta_3) = -9.95$  dB.

TABLE 1

Simulation 1 output for array gain at jammer positions and the ratio of individual jammer power to white noise power at the radar output

M	$G(\theta_q)$ (dB)	$\ell$	$f_{\ell}$	$\theta_{\ell}$ (degree)	$P_{\ell}$ (dB)	$G(\theta_{\ell})$ (dB)	$P_{\ell}G(\theta_{\ell})/\sigma^2\eta$ (dB)
0	10	1	1	-17	0	- 3.00	37.00
		2	1	30	-10	- 6.99	23.01
		3	1	65	-20	- 9.95	10.05
1	9.88	1	1	-17	0	-12.80	27.20
		2	1	30	-10	- 4.58	25.42
		3	1	65	-20	- 8.56	11.44
2	9.70	1	1	-17	0	-29.50	10.50
		2	1	30	-10	-29.72	0.28
		3	1	65	-20	- 9.20	10.80
3	9.66	1	1	-17	0	-38.17	1.83
		2	1	30	-10	-44.49	< 0
		3	1	65	-20	-23.84	< 0

The ratio of individual jammer power to white noise power at the output of the radar was calculated as  $P_{\ell}G(\theta_{\ell})/\sigma_{\eta}^2$ . These values were 37.00 dB, 23.01 dB and 10.05 dB for the three jammers. Array gain patterns calculated at  $0.5^\circ$  intervals with  $M=1,2$  and 3 are plotted in Figures 3 to 5. After adaptation with one noise vector, the gain in the direction of the strongest jammer was reduced by 9.80 dB to  $G(\theta_1) = -12.80$  dB. At the same time,  $G(\theta_2)$  and  $G(\theta_3)$  were increased slightly. With two noise vectors, the gains in the directions of the first two strongest jammers were reduced by 26.50 dB and 22.73 dB respectively to  $G(\theta_1) = -29.50$  dB and  $G(\theta_2) = -29.72$  dB. Gain  $G(\theta_3)$  was slightly above the value calculated with  $M=0$ . When the number of noise vectors was equal to the number of jammers, the output power of the strongest jammer was reduced to 1.83 dB above the white noise background. Those of the other jammers were below this background.

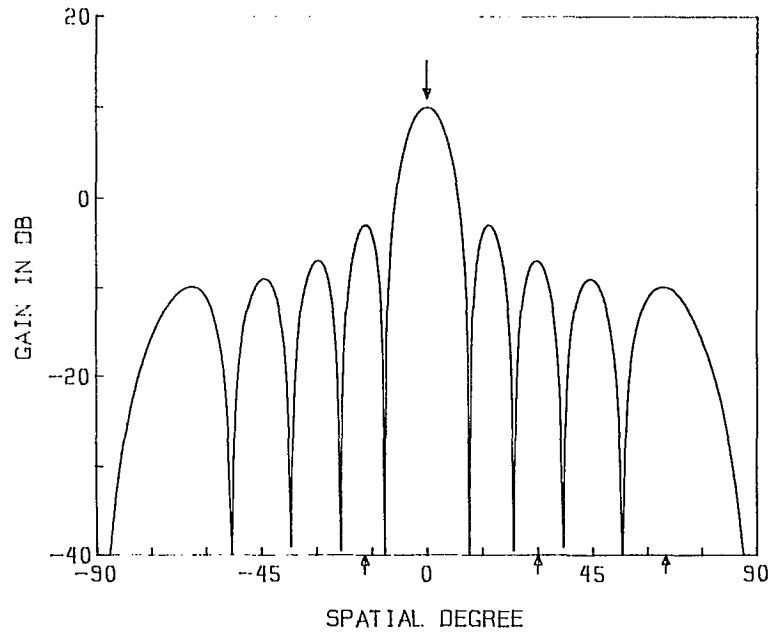


Figure 2. Quiescent gain pattern in Simulation 1. The beam pointing direction  $\theta_q$  is marked with an arrow above the gain at  $\theta_q=0$ . Jammer positions are marked with arrows below the x-axis.

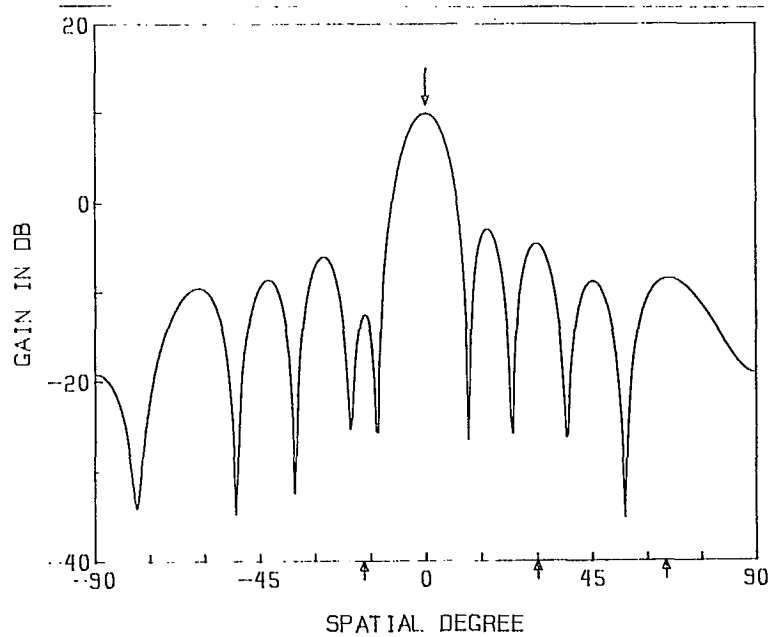


Figure 3. Simulation 1 gain pattern calculated with one noise vector. Jammer powers from left to right are 40 dB, 30 dB, and 20 dB above the white noise background.

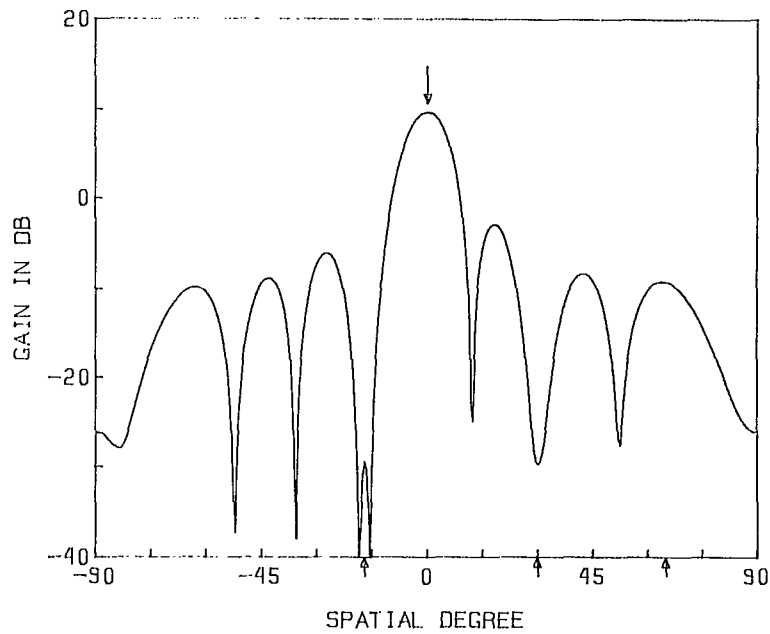


Figure 4. Simulation 1 gain pattern calculated with two noise vectors

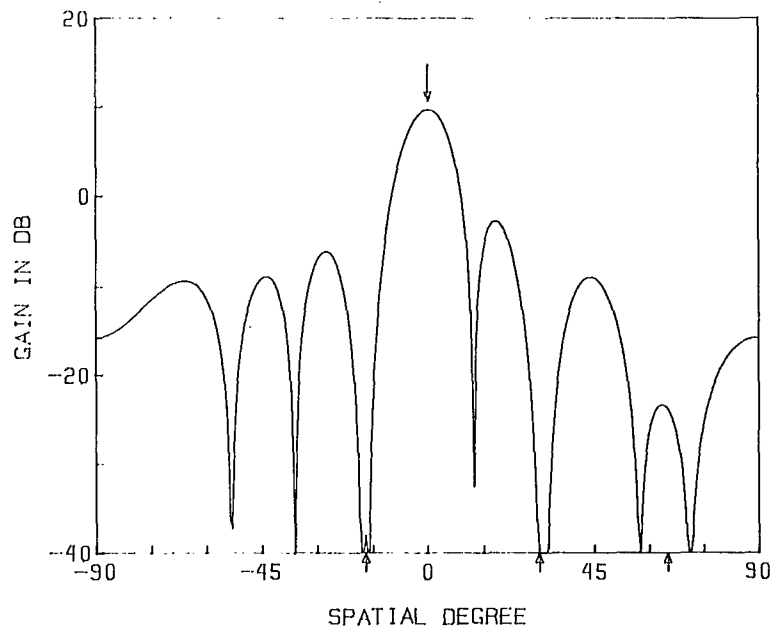


Figure 5. Simulation 1 gain pattern calculated with three noise vectors

### 3.3 SIMULATION 2

This simulation studied the performance of the jammer suppression algorithm in the presence of a band jammer. The simulation parameters were  $K=10$ ,  $\theta_q=0^\circ$ ,  $f=1.0$ ,  $L=21$ ,  $P_\ell=1$ ,  $f_\ell = 0.989 + 0.001\ell$ ,  $\theta_\ell = -17^\circ$ ,  $\sigma_\eta^2 = 10^{-4}$ ,  $\Delta = 4K\sigma_\eta^2$ , and  $M=0$  and  $1$ . Here, the band jammer was positioned at  $-17^\circ$  and was constructed as a sum of 21 jammers ranging in frequencies from 99% to 101% of the radar design frequency. Array gains were calculated at the radar design frequency, using  $M=0$  and  $1$ .

The results of this simulation are summarized in Table 2 which contains the values of  $P_\ell G(\theta_\ell)/\sigma_\eta^2$  for  $\ell = 1, 2, \dots, \text{ and } 21$ , and for  $M=0$  and  $1$ , using the  $G(\theta_\ell)$ 's calculated with  $f = f_\ell$  in (19). The sum of these values for a given  $M$  was the ratio of total jammer power to white noise power at the radar output. This ratio was 50.2 dB before adaptation. After adaptation with only one noise vector, it was reduced by 45.6 dB to 4.6 dB. The array gain pattern, calculated with  $M=1$  and  $f=1.0$ , is presented in Figure 6. The gain is below -40 dB at the jammer position. Gain patterns had also been calculated with  $(M=1, f=0.99)$  and  $(M=1, f=1.01)$ . These patterns are not presented here, because they were almost indistinguishable from the pattern in Figure 6.

TABLE 2

Simulation 2 output for the ratio of jammer power to white noise power before and after adaptation with one noise vector

$\ell$	$f_\ell$	$P_\ell G(\theta_\ell)/\sigma_\eta^2$	
		$M=0$	$M=1$
1	0.990	5043	0.3526
2	0.991	5042	0.3280
3	0.992	5040	0.3031
4	0.993	5037	0.2781
5	0.994	5035	0.2533
6	0.995	5032	0.2286
7	0.996	5029	0.2044
8	0.997	5026	0.1806
9	0.998	5023	0.1577
10	0.999	5020	0.1355
11	1.000	5016	0.1144
12	1.001	5012	0.0945
13	1.002	5008	0.0760
14	1.003	5004	0.0590
15	1.004	4999	0.0439
16	1.005	4995	0.0306
17	1.006	4990	0.0196
18	1.007	4985	0.0109
19	1.008	4979	0.0047
20	1.009	4974	0.0013
21	1.010	4968	0.0010
21		105257	2.8778
$\sum_{\ell=1} P_\ell G(\theta_\ell)/\sigma_\eta^2$		(50.2 dB)	(4.6 dB)



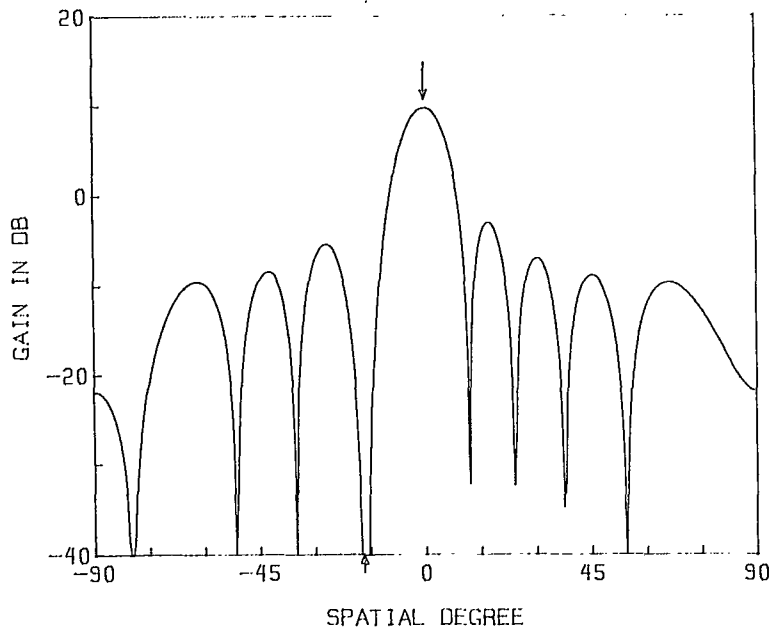


Figure 6. Simulation 2 gain pattern calculated with one noise vector. There are 21 jammers at  $\theta = -17^\circ$ . Jammer frequencies range from 99% to 101% of design frequency. Quiescent gain pattern is given by Figure 2.

### 3.4 SIMULATION 3

This simulation studied the performance of the algorithm in the presence of a cluster of jammers. The simulation parameters were  $K=10$ ,  $\theta = 0^\circ$ ,  $f=1$ ,  $L=21$ ,  $P_\ell=1$ ,  $f_\ell=1$ ,  $\theta_\ell = -15.9-0.1\ell$  degree,  $\sigma_\eta^2 = 10^{-4}$ ,  $\Delta=4K\sigma_\eta^2$ , and  $M=0,1,2$ , and 3. Here, the cluster was centred at  $-17^\circ$  and was constructed as a sum of 21 jammers ranging in positions  $-16.0$  to  $-18.0^\circ$ . Array gains were calculated with up to three noise vectors.

The results of this simulation are summarized in Table 3. The ratio of total jammer power to white noise power at the radar output was 50.1 dB before adaptation. This ratio was reduced by 27.2 dB to 22.9 dB after adaptation with one noise vector. The ratios were 15.3 dB and 9.0 dB with  $M=2$  and  $M=3$  respectively. The array gain pattern, calculated with  $M=1$ , is presented in Figure 7.

## 4. CONCLUSIONS

The derivation of an adaptive jammer suppression algorithm using the Gram-Schmidt orthonormalization method has been presented. The number of add and multiply operations in this algorithm is proportional to the number of elements in the array. Computer simulations also show that very few noise samples are needed in order to reduce the powers of individual jammers to

TABLE 3

Simulation 3 output for the ratio of jammer power to white noise power. Calculations were made with up to three noise vectors.

$\ell$	$\theta_\ell$	$P_\ell G(\theta_\ell)/\sigma_\eta^2$			
		M=0	M=1	M=2	M=3
1	-16.0	4888	18.66	5.280	0.508
2	-16.1	4932	18.87	3.939	0.482
3	-16.2	4970	18.78	2.899	0.476
4	-16.3	5000	18.38	2.101	0.476
5	-16.4	5023	17.60	1.494	0.473
6	-16.5	5039	16.73	1.039	0.459
7	-16.6	5048	15.52	0.700	0.433
8	-16.7	5050	14.11	0.451	0.391
9	-16.8	5046	12.53	0.273	0.336
10	-16.9	5034	10.82	0.153	0.271
11	-17.0	5016	9.05	0.086	0.201
12	-17.1	4991	7.27	0.071	0.132
13	-17.2	4960	5.54	0.115	0.073
14	-17.3	4923	3.92	0.227	0.034
15	-17.4	4879	2.49	0.425	0.024
16	-17.5	4830	1.32	0.728	0.055
17	-17.6	4775	0.48	1.161	0.139
18	-17.7	4714	0.05	1.754	0.290
19	-17.8	4648	0.11	2.537	0.519
20	-17.9	4577	0.74	3.545	0.840
21	-18.0	4502	2.01	4.817	1.267
21		102845	195.07	33.795	7.879
$\sum_{\ell=1} P_\ell G(\theta_\ell)/\sigma_\eta^2$		(50.1 dB)	(22.9 dB)	(15.3 dB)	(9.0 dB)

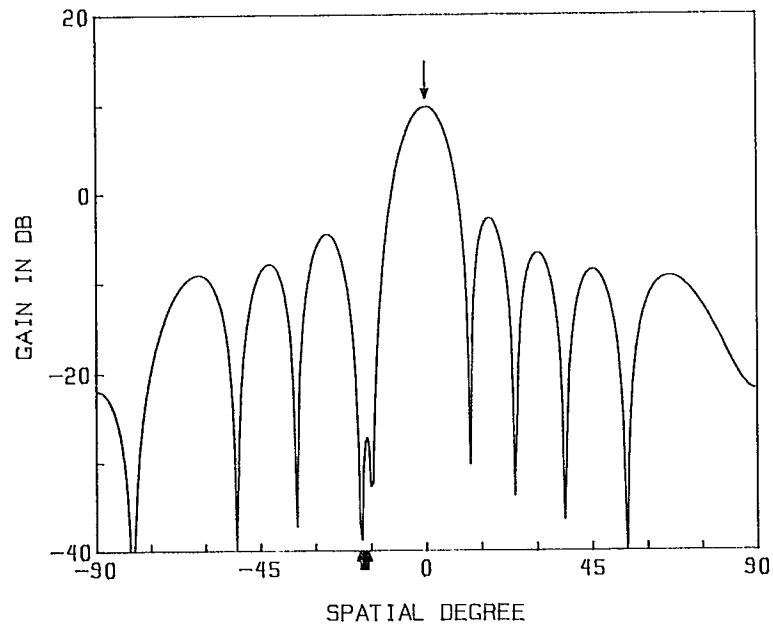


Figure 7. Simulation 3 gain pattern calculated with one noise vector. There are 21 jammers in the range  $\theta = -16^\circ$  to  $-18^\circ$ . Quiescent gain pattern is given by Figure 2.

less than 10 dB above the power of the white noise background. Further studies of this algorithm should include the use of vectors in the covariance matrix instead of noise vectors in the algorithm procedure.

## 5. ACKNOWLEDGEMENT

This work was supported by the Department of National Defence under Research and Development Branch Project 33C69.



